CONFERENCE PRE-PRINT

HOW MEV-RANGE IONS AND HIGH β WILL SHAPE THE CORE PLASMA DYNAMICS OF FUSION POWER PLANTS

S. MAZZI
CEA, IRFM
Saint Paul-lez-Durance, France
Email: samuele.mazzi@cea.fr

J. GARCIA, G. GIRUZZI, R. DUMONT
CEA, IRFM
Saint Paul-lez-Durance, France

Y. KAZAKOV, J. ONGENA
Laboratory for Plasma Physics, LPP-ERM/KMS
Brussels, Belgium

D. ZARZOSO
Aix Marseille Université, CNRS, Centrale Med, M2P2
Marseille, France

F. P. ORSITTO
ENEA Department Fusion and Technology for Nuclear Safety, C.R. Frascati
Frascati, Italy

E. DE LA LUNA
National Fusion Laboratory, CIEMAT
Madrid, Spain

L. SENNI
Istituto per le Applicazioni del Calcolo 'Mauro Picone', CNR
Rome, Italy

M. FONTANA
Tokamak Energy Ltd.
Abingdon, United Kingdom

S. BRUNNER
Ecole Polytechnique Fédérale de Lausanne (EPFL), Swiss Plasma Center (SPC)
Lausanne, Switzerland

M. DREVAL
Institute of Plasma Physics, National Science Center, Kharkiv Institute of Physics and Technology
Kharkiv, Ukraine

J. VARELA
Institute for Fusion Studies, Department of Physics, University of Texas at Austin
Austin, Texas, USA

J. RUIZ RUIZ
Rudolf Peierls Centre for Theoretical Physics, University of Oxford
Oxford, UK

A. ZOCCO
Max-Planck-Institut fur Plasmaphysik, EURATOM Association
Greifswald, Germany

JET CONTRIBUTORS
see the author list of C.F. Maggi et al., Nucl. Fusion 64, 112012 (2024)

WPTE TEAM
see the author list of E. Joffrin et al., Nucl. Fusion 64, 112019 (2024)

TCV TEAM
see the author list of B. P. Duval et al., Nucl. Fusion 64, 112023 (2024)

Aabstract

Next-generation fusion power plants will operate in burning plasma regimes characterized by high β and dominant heating by fusion-born α particles. In such conditions, the core plasma dynamics are governed by the nonlinear interplay of MeV-range ions, Alfvénic instabilities, microturbulence, and strong electromagnetic fluctuations. The paper integrates recent experimental and theoretical results to show that turbulence suppression triggered by fast ions and the emergence of high-β KBM-induced distortions in the electron distribution function (EDF) are two facets of a strongly coupled system. Evidence from various tokamak experiments and advanced numerical modelling demonstrates how fast-ion-driven Alfvén modes regulate turbulence through zonal structures, while high-β KBMs lead to bipolar perturbations in the EDF that may affect the measurement of key diagnostics such as the electron cyclotron emission (ECE) radiometers. The coexistence and mutual reinforcement of these mechanisms have profound implications for confinement optimization, performance assessment, and diagnostic interpretation in future fusion reactors.

1. INTRODUCTION

The fusion of deuterium and tritium in magnetically confined plasmas offers a path to clean, virtually limitless energy. Among confinement device concepts, tokamaks are the most advanced, using toroidal and poloidal magnetic fields to sustain high-temperature plasmas. Achieving ignition conditions in magnetically confined plasmas requires external heating sources such as Neutral Beam Injection (NBI) and Ion Cyclotron Resonance Heating (ICRH). These mechanisms generate fast ions, i.e. particles with energies significantly exceeding those of the bulk plasma. In addition, fusion reactions themselves produce energetic alpha particles. While fast ions play a crucial role in plasma heating and to sustain the fusion reaction, they can also excite high-frequency instabilities, such as Alfvén eigenmodes (AEs) and Energetic Particle Modes (EPMs), which may lead to confinement degradation [1].

External heating also produces steep temperature and density gradients, which can destabilize microinstabilities at the ion Larmor radius scale, particularly ion temperature gradient (ITG) modes and the Kinetic Ballooning Modes (KBMs), driving turbulence and anomalous transport that limits energy confinement. Interestingly, experiments and simulations have shown that fast ions can suppress ion-scale turbulence, mainly driven by ITG, enhancing confinement and performances through many different mechanisms (see [2–5]). In particular, a multiscale nonlinear mechanism involving fast-ion-driven AEs have been recently reported to strongly affect the core-turbulence intensity by suppressing it and achieve optimum confinement [6], also in DT plasmas [7]. Gyrokinetic simulations unveiled the fine underlying physics of such a beneficial mechanism [8–11], including the coupling to an enhanced zonal flow activity. This latter point has also been recently demonstrated experimentally [12], corroborating thus once more the validity of the first-principle numerical analysis. Moreover, this mechanism is not reserved only to AEs, but also EPMs, such as fishbones, can generate strong zonal flow activity impacting therefore on the plasma performances [13].

Understanding fast-ion–turbulence interactions is critical for future burning plasma scenarios, where MeV-range alpha particles dominate the core dynamics, and such improved confinement may be reached by exploiting the fast-ion-triggered beneficial mechanism. Connected to this, high-performance plasmas, with high pressure in the plasma core (and thereby high β, where β is the ratio between the thermodynamical and the magnetic pressure) are also frequently obtained in current tokamaks, both in DD and DT plasmas. The same kind of results are envisaged for the next-generation tokamaks, and hence it is of paramount importance to determine the physical properties of the deep-core under high-performance plasma conditions. Due to the difficulties in reaching these internal positions of the plasma through routinely used diagnostics, advanced numerical simulations represents a crucial tool to explore the deep-core of the high-performance plasmas. In these conditions, KBMs have been found unstable, possibly determining the pressure profile shapes [14–16].

In this manuscript, these findings are reconciled an synthesized into a coherent picture of the nonlinear plasma core dynamics, focusing on two tightly intertwined aspects: (i) the confinement properties regulation by MeV-range ions destabilizing AEs and their coupling to zonal structures, and (ii) the destabilization of KBMs at high β, which deform the EDF and bias specific diagnostic measurements. These two aspects cannot be separated into a linear chain of causes and effects, but instead form a nonlinear set of interactions, where fast-ion-driven instabilities, turbulence, and electromagnetic fluctuations coexist and evolve consistently.

2. NONLINEAR FAST-ION-TRIGGERED REGULATION OF TURBULENCE PROPERTIES

This section addresses how fast-ion-driven AEs interact with zonal flows and structures to influence turbulence and improve plasma confinement in tokamaks. Motivated by experimental observations from JET showing unexpected reduction of thermal ion transport, theoretical and numerical analyses have focused on the role of fast ions in regulating background turbulence.

Flux-tube gyrokinetic simulations with the GENE code [17] on selected L-mode JET pulses demonstrated that introducing fast ions in nonlinear electromagnetic simulations significantly reduces the thermal ion heat flux [18], predominantly affecting nonlinear dynamics and ruling out thus purely linear mechanisms. Subsequent studies on JET H-mode pulses examined how fast-ion content can affect the thermal transport but also influence the critical β threshold for high-frequency pressure-driven modes (such as KBMs and/or Beta Alfvén Eigenmodes) [19]. Nonlinear simulations showed that turbulence reduction arises from a synergy between fast-ion pressure effects and electromagnetic stabilization, particularly close to marginality of the onset of fast-ion-driven high-frequency modes [19]. As in those plasma no high frequency modes destabilized by fast ions were observed experimentally (and also to avoid flux runaway in the gyrokinetic simulations), the fast-ion pressure gradients were ad-hoc modified below the critical value.

Such a near-marginality of the fast-ion-driven modes was fundamental to explain the underlying physics leading to the reduced ion turbulent fluxes. Indeed, the linearly stable Toroidal Alfvén Eigenmodes (TAEs) are destabilized nonlinearly by energy depletion from the ITG scales toward the large fast-ion scales [8]. The TAEs, in turn, couple and transfer energy to the zonal components of the electrostatic potential. Such an enhanced zonal flow activity counteracts on the ITG-driven turbulent fluxes, reducing their saturation toward very low levels, compatible with the experimentally-inferred thermal transport ones.

It was however observed that a runaway character of the energy fluxes (mainly for the electron and fast ion components) appears when the TAEs are linearly unstable, limiting their beneficial impact up to the critical destabilizing β [8]. The experimental demonstration of this numerical study was thereby missing, as no TAEs were experimentally detected in the analyzed JET pulse #73224.

The experimental demonstration of such a beneficial mechanism triggered by fast-ion-driven TAEs has been recently provided in the 3-ion heating scheme scenario at JET [20], in which an efficient combination of NBI (8 MW) and ICRH (6 MW) leads to the generation of a significant population of MeV-range ions in the deep plasma core of pulse #94701 [21]. Those ions, thanks to their high energy, destabilize a rich activity of high-frequency instabilities, among which the TAEs are present in the plasma core, where a clear enhanced confinement, especially for the thermal ions, is measured [6]. Gyrokinetic flux-tube simulations with the GENE code reveal the underlying complex mechanism, describing cross-scale multi-mode interactions leading to such an improved thermal ion confinement. Interestingly, in this specific study, the maximum of the turbulence reduction is obtained in conditions with linearly unstable TAEs, as can be observed in Fig. 1 for the cases with fast ion pressure gradients large enough to destabilize the TAEs. The almost complete suppression of the thermal ion fluxes (with respect to the artificial case without including fast ions) is reached due to a strong zonal flow activity, which acts as a reservoir of energy and also as a shearing turbulence medium. The enhanced amplitude of the zonal structures, for both the electrostatic and the magnetic potential, is directly caused by the multi-scale energy transfer from the TAE to their meso-scale. Bispectral analysis, whose main results are illustrated in Fig. 2, is defined as:

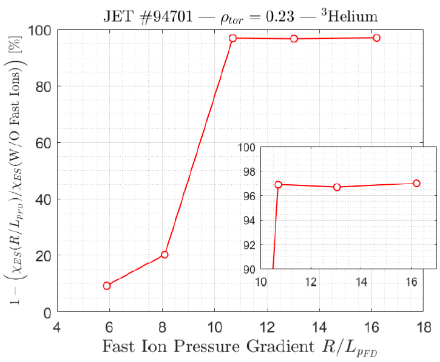

FIG. 1. The relative reduction of the ^{3}He electrostatic heat diffusivities with respect to the case without fast ions is plotted as a function of the fast ion pressure gradient $R/L_{p_{FD}}$ from GENE simulations for JET pulse #94701.

$$b^W(f', f'') = \left| \int \mathrm{d}t \sum (\phi_{k_y}(f,t))^\dagger \times \phi_{k_y'}(f',t)\phi_{k_y''}(f'',t) \right| \tag{1}$$

with ϕ the electrostatic potential, k_y the selected binormal wavenumber and $\dagger$ representing the complex conjugate. It can, thus, highlight such an interaction occurring at the intersection of the zonal flow frequency (i.e. f=0) and the TAE frequency (f $\sim$200 kHz). This coupling has also been validated experimentally in a recent study, in which the Doppler Backscattering reflectometer measurements of density fluctuations clearly unveiled a wave-wave coupling between the zero-frequency zonal flows and the TAEs (and all the harmonics) in the same 3-ion scheme scenario at JET [12].

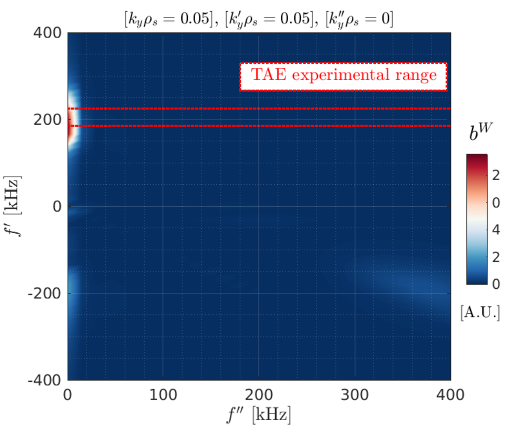

FIG. 2. Bispectrum of the electrostatic potential fluctuations for the triad of the most destabilized TAE mode ($k'_y = 0.05$), the zonal components ($k''_y = 0$) and the modes completing the triplets ($k_y = 0.05$), for the case with $R/L_{p_{FD}} = 13.6$. The TAE experimental range of frequencies is highlighted with red horizontal dotted lines.

Also, the zonal components of the magnetic potential are enhanced by such an interaction with the TAE scales; nonetheless their impact on the turbulence properties is not fully understood, although an enhanced zonal field activity may act on the local magnetic profile characteristics, modifying the safety factor and/or the magnetic shear affecting thereby the whole stability picture.

An additional analysis unveil the role of the cross-phase angle among the main plasma parameters composing the kernel of the energy flux calculation, i.e. the electrostatic potential ϕ and the ion temperature fluctuations $\tilde{T}_\parallel$ and $\tilde{T}_\perp$. The definition of the cross-phase angle is:

$$\alpha(A \times B) = \tan^{-1}\big(Im(A/B)/Re(A/B)\big) \tag{2}$$

with A and B thereby representing a combination of the three parameters listed above. For the sake of clarity, when the two parameters are out-of-phase ($\alpha = \pm\pi/2$) the fluxes are maximized, with respect to the in-phase cases ($\alpha = \pm\pi$ or 0). It is observed in the gyrokinetic simulations that, when the TAEs trigger the complex multi-scale interaction, a signature in the cross-phase structures is clearly visible. This is shown in Fig. 3, for simplicity only for the $\alpha(\phi \times \tilde{T}_\parallel)$, in which the TAE destabilization leads to a regime transition from a ITG- to a TAE-scale structure, and more importantly from an out-of-phase structure to a in-phase one. This picture is therefore consistent with the suppressed thermal ion flux obtained in the simulations, despite the general increased amplitude of the electro-magnetic field fluctuations. Similar effects are also observed in other study cases [11, 22], and could open the way to an additional experimental validation method for such a beneficial mechanism.

Following these results, a dedicated scenario with dominant ICRH minority heating (~1% H in 50-50% DT fuel) in the DTE2 campaign has been designed and performed in order to exploit the improved confinement previously observed in plasmas with fast-ion-driven TAEs. This configuration successfully reproduced rich AE activity, dominant electron heating, and low torque, similarly to the previous 3-ion scheme scenario [7]. Nevertheless, the DT plasmas exhibited richer MHD dynamics, including TAEs, Fishbones, and NTMs, with clear nonlinear interactions. Despite these instabilities, the reference pulse (#99896) achieved a better confinement than the matched (from the engineering parameters) DD case (#100871), with the formation of an edge pedestal without ELMs and evidence of an isotope effect from tritium, manifesting as reduced core diffusivity and enhanced pedestal height with respect to the DD case.

Extensive simulations confirmed that TAEs were not driven by fusion-born alphas but by ICRH-generated ions. FAR3D [23] modelling showed that TAEs efficiently transfer energy to zonal flows, reinforcing turbulence suppression. Gyrokinetic CGYRO [24] analyses confirmed the FAR3D results and additionally revealed that turbulence stabilization was highly sensitive to fast-ion parameters: reducing the T_{fast}/T_e ratio or reducing $R/L_{p_{FD}}$ significantly weakened the turbulence reduction [7]. Thus, linearly unstable TAEs were identified as a necessary condition for reproducing experimentally observed transport levels.

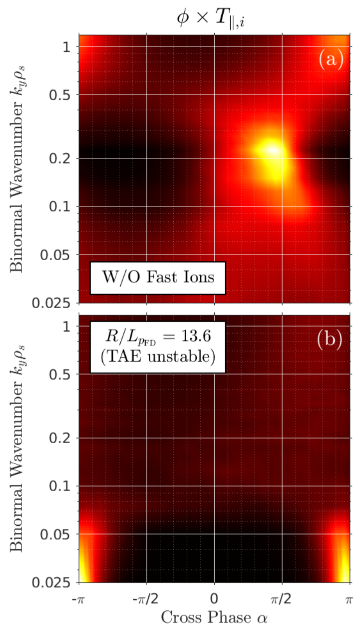

FIG. 3. Simulated cross phase between electrostatic potential and parallel ion temperature fluctuations without fast ions (a) and with unstable TAE (b).

Recent experiments, following the sparked interest of the JET results, corroborate these observations of improved confinement in the presence of fast-ion-driven TAEs (in those experiments the fast ion are generated by the NBI) [25, 26].

3. KBM SHAPING THE CHARACTERISTICS OF HIGH BETA DEEP-CORE PLASMAS

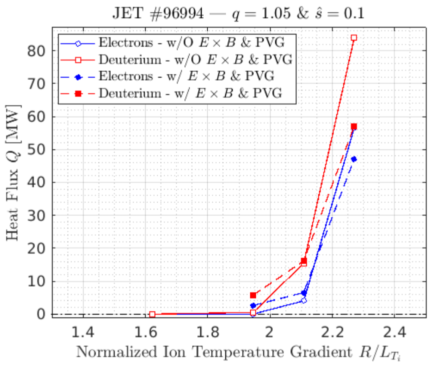

FIG. 4. Electron (blue) and thermal ion Deuterium (red) heat flux for different values of the normalized ion temperature gradient R/L_{T_i}, in the configurations with (dashed) and without (solid) $E \times B$ and parallel velocity gradient PVG.

In high-β plasma regions, as the deep core of high-performance plasmas, nonlinear flux-tube gyrokinetic simulations have demonstrated that localized KBMs can simultaneously determine the turbulent transport threshold [14, 15] and strongly perturb the EDF [16]. Indeed, in high-performance JET pulses, KBMs were found to dominate the transport when the electron β (β_e) exceeds a critical threshold, with their saturation level determining the magnitude of turbulent total heat fluxes. The KBMs are however destabilized only at low magnetic shear, thereby demonstrating a clear impact of the local magnetic equilibrium on the linear growth rate [15, 16]. Concerning the nonlinearly computed heat transport, a very large stiffness is observed, with a clear implication on the local profile shape that can be achieved. The stiffness of the heat fluxes determined by the destabilization of the core-KBMs is shown in Fig. 4.

Importantly, the gyrokinetic simulations of the high-temperature JET pulse #96994 [27] revealed that the unstable KBMs have a clear impact on the linear EDF shape in the momentum p space. This is shown in the panels Fig. 5, in which the GENE-computed perturbed EDFs are shown in the momentum space for a KBM-dominated binormal wavenumber and for different electron profile local gradient configurations. A bipolar structure clearly appears, determining a non-Maxwellian shape for the perturbed EDF.

It is also observed that the structure moves in the electron momentum space according to the normalized electron diamagnetic frequency ω_e^*:

$$\omega_e^* = \left[R/L_{n_e} + R/L_{T_e}\left(p_\parallel^2 + p_\perp^2 - \frac{3}{2}\right)\right]\frac{T_e k_y}{eB_0 a} \tag{3}$$

where R/L_{n_e} and R/L_{T_e} are the local normalized electron density and temperature gradients, respectively, and a and R the minor and major radii, respectively. The mechanism underlying this EDF modification is a resonant wave–particle interaction: electrons with diamagnetic frequency ω_e^*, determined by the local density and temperature gradients, interact with KBMs at their characteristic frequency ω_{KBM}. As a result, the EDF in momentum space $(p_\parallel, p_\perp)$ acquires a distinctive bipolar structure, centered at $\omega_e^* = 0$ and peaking at $\omega_e^* \approx \omega_{\mathrm{KBM}}$. Electrons with orbits such that their diamagnetic drift matches the KBM frequency are selectively enhanced or depleted, producing positive and negative deviations around the thermal momentum scale.

This dependence is displayed in the different panels of Fig. 5, in which the diamagnetic frequency has been modified by varying R/L_{n_e} and R/L_{T_e}. It is observed, hence, that $\omega_e^* = 0$ (represented by the black dashed contour lines) robustly matches the localization where the perturbed EDF is null (green solid lines), while the bump region of the distribution (bordered by the yellow dotted lines) clearly overlaps with the value of $\omega_e^* = \omega_{\mathrm{KBM}}$. And for the dif-

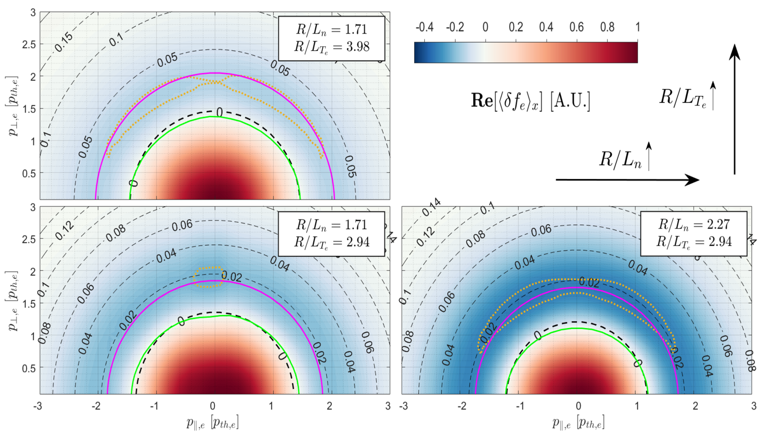

FIG. 5. Normalized linear perturbed electron distribution function δf_e for the KBM-dominated $k_y\rho_s = 0.02$ for different combinations of R/L_{n_e} and R/L_{T_e}. The black dashed lines represent ω_e^*, the pink curve the normalized KBM frequency, while the green solid and yellow dashed curves are respectively the position of $\delta f_e = 0$ and the minimum of δf_e.

ferent configurations of the electron profiles, the match is always fulfilled. Quantitatively, these bipolar perturbations reach in the nonlinear phase a few percent of the equilibrium EDF ($\approx$ 2–3% in analyzed JET conditions), which is sufficiently large to modify radiative properties of the plasma core. Moreover, the amplitude of the bipolar structure lobes and the radial localization of the KBM structure in the poloidal section strongly depend on the KBM-induced turbulence intensity in the nonlinear phase. This is shown in Fig. 6, in which the radial extent of the KBM-induced structure in the temperature fluctuations is enlarged with the increase of the KBM drive R/L_{T_i}, but are nonetheless still fairly localized ($\sim$15 cm). Nevertheless, as discussed before, the KBM heat flux evolution is very stiff, and thus a limitation to the reachable KBM drive is determined by the experimentally inferred levels of radial transport. The spatial localization of KBMs ensures that the strongest EDF perturbations occur in the inner radial region, where β_e and pressure gradients are highest.

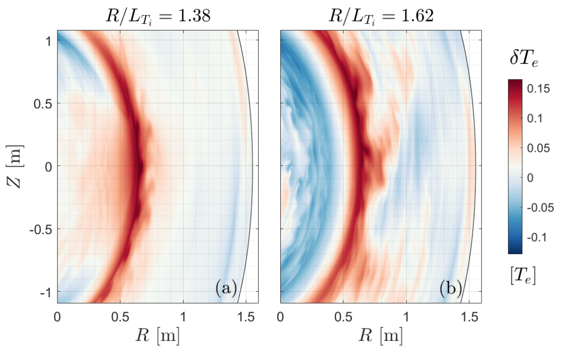

FIG. 6. The poloidal representation of KBM-induced temperature fluctuations computed by the nonlinear code GENE for two different KBM drives. The radial coordinate has been normalized to be 0 at the inner boundary of the numerical box.

These insights extend the role of KBM beyond its impact on transport: KBM can act as a kinetic agent that imprints non-Maxwellian signatures in the EDF, bridging turbulence and diagnostic observables. In fact, the bipolar distortion of the EDF aligns well in ampltiude, shape and position with the heuristic model [28] previously proposed to explain the long-standing discrepancy between Electron Cyclotron Emission (ECE) and Thomson Scattering (TS) measurements. This discrepancy arises due to the ECE sensitivity to the shape of the EDF [29], and the bipolar structure characteristics can be fine-tuned to reconcile the two measurements for different multiple scenarios and pulses. This has been done for a substantial JET database of recent high temperature plasmas, and the reader is addressed to Ref. [28] for more details on the database and on the heursitic model for reconciliation of the ECE-TS discrepancy. Importantly, the shape of the bipolar EDF perturbation produced by KBMs closely matches the bipolar form assumed in the heuristic model for the JET pulse #96994, as shown in Fig. 7. In panel (a) of the figure, the ECE vs. TS measurements are compared, clearly denoting a discrepancy between the two, mainly for $T_e > 4 - 5$ keV. The heuristic model, by

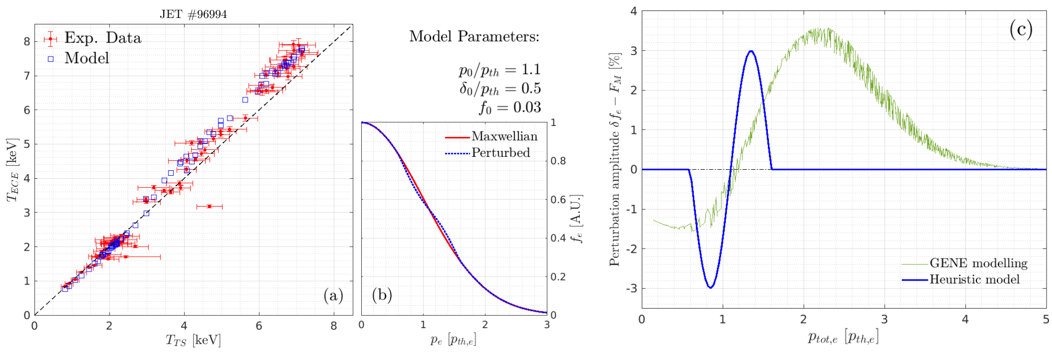

FIG. 7. (a) Comparison between TS and ECE measurements for JET pulse #96994. The red squares represent the ECE-measured T_e including the perturbed EDF of the heuristic model displayed in panel (b), with the explicit parameters employed in the heuristic model, i.e. p_0 the center position, δ_0 the extension along the total momentum and f_0 the amplitude of the perturbation. In (c) the KBM-induced perturbation as computed by GENE is compared to the one of the heuristic model.

introducing the pertubation illustrated in panel (b), clearly reconcile the discrepancy (red square in panel (a)). If the same perturbation is compared to the one generated by the KBM in GENE calculations (panel(c)), a good agreement is obtained, especially for the localization in the momentum space of the bipolar center around the thermal velocity.

4. DISCUSSION AND WRAPPING UP

This work has highlighted two key ingredients that will shape the dynamics of reactor-relevant burning plasmas: the role of MeV-range ions (a.k.a. fusion-born alpha particles) in regulating turbulence through the destabilization of the Alfvénic activity, and the impact of KBMs on the EDF in the plasma core. Although presented in separate sections, these processes are not independent, but rather they represent two components of a nonlinear and self-consistent deep-core plasma condition.

On one side, fast ions destabilize Toroidal Alfvén Eigenmodes (TAEs) which, through nonlinear multi-scale and multi-mode interactions, transfer energy to the zonal structures. This enhanced zonal activity suppresses the background ion-scale turbulence, leading to significantly reduced thermal transport and improved confinement, as demonstrated in JET experiments and validated gyrokinetic simulations. The beneficial effect of fast-ion-driven modes can steepen core pressure gradients and increase the overall β of the plasma, thereby leading the system closer to the KBM threshold.

On the other side, once the plasma enters such high-β regimes, KBMs become linearly unstable and dominate the transport, leading to a strong stiffness of the heat fluxes. Equally important, KBM-driven wave–particle interactions with electrons modify the EDF in momentum space, generating a bipolar distortion localized around the thermal velocity of the electrons. A clear dependence on the electron diamagnetic frequency is demonstrated, with the structure moving in the momentum space accordingly to the relation:

$$p_0 = \sqrt{\frac{3}{2} - \frac{R/L_{n_e}}{R/L_{T_e}}} \tag{4}$$

which has been directly derived from Relation 3 and illustrates clearly the dependence of the center position of the bipolar structure p_0 in the momentum space on the local shape of the electron profiles. The KBM-induced perturbations, although of only a few percent amplitude, are sufficient to alter the spectral properties of the ECE and thus impair the temperature measurements with the ECE radiometers. The fact that the KBM-induced EDF distortion closely reproduces the bipolar shape proposed in a recent heuristic model [28] to reconcile the ECE–TS discrepancy provides a strong physical basis for understanding this long-standing issue, which is currently being deeply investigated by a dedicated task-force under the ITPA framework [30]

The interplay between these two mechanisms is of particular importance for next-generation fusion reactors, such as ITER, SPARC and DEMO for instance. Improved confinement via fast-ion-driven AEs increases the pressure gradients in the plasma core, favoring the KBM destabilization and associated EDF perturbations. In turn, these distortions directly affect the diagnostic measurements used to evaluate performance, which may introduce large uncertainties in the evaluation of electron temperature profiles; nonetheless, it also open the path to the use of the ECE as a tool to determine the KBM-induced turbulence properties in the plasma core through the evaluation of the perturbation position in the momentum space combined with the measurement of the local electron profiles via Relation 4.

ACKNOWLEDGEMENTS

This work has been carried out within the framework of the EUROfusion Consortium, funded by the European Union via the Euratom Research and Training Programme (Grant Agreement No 101052200 — EUROfusion). Views and opinions expressed are however those of the author(s) only and do not necessarily reflect those of the European Union or the European Commission. Neither the European Union nor the European Commission can be held responsible for them.

REFERENCES

[1] M Salewski et al. Energetic particle physics: Chapter 7 of the special issue: on the path to tokamak burning plasma operation. *Nuclear Fusion*, 65(4):043002, 2025.

[2] J. Citrin and P. Mantica. Overview of tokamak turbulence stabilization by fast ions. *Plasma Physics and Controlled Fusion*, 65(3):033001, 2023.

[3] J. Garcia and JET Contributors. Electromagnetic and fast ions effects as a key mechanism for turbulent transport suppression at JET. *Plasma Physics and Controlled Fusion*, 64(10):104002, 2022.

[4] Y.-S. Na et al. How fast ions mitigate turbulence and enhance confinement in tokamak fusion plasmas. *Nature Reviews Physics*, 7:190–202, 2025.

[5] S. Mazzi et al. Fast ion interaction with turbulence mediated by zonal flows in tokamak plasmas: Overview of the recent insights. *Submitted to Reviews of Modern Plasma Physics*, 2025.

[6] S. Mazzi et al. Enhanced performance in fusion plasmas through turbulence suppression by megaelectronvolt ions. *Nature Physics*, 18(7):776–782, 2022.

[7] J. Garcia et al. Stable deuterium-tritium plasmas with improved confinement in the presence of energetic-ion instabilities. *Nature Communications*, 15(1):7846, 2024.

[8] A. Di Siena et al. Electromagnetic turbulence suppression by energetic particle driven modes. *Nuclear Fusion*, 59(12):124001, 2019.

[9] S. Mazzi et al. Gyrokinetic study of transport suppression in JET plasmas with MeV-ions and toroidal Alfvén eigenmodes. *Plasma Physics and Controlled Fusion*, 64(11):114001, 2022.

[10] J. N. Sama et al. Ion temperature gradient mode mitigation by energetic particles, mediated by forced-driven zonal flows. *Physics of Plasmas*, 31(11), 2024.

[11] A. Di Siena et al. Understanding turbulence suppression in JET D-T plasma with MeV fast ions via global gyrokinetic GENE simulations. *Nuclear Fusion*, 2025.

[12] J. Ruiz Ruiz et al. Measurement of zero-frequency fluctuations generated by coupling between alfvén modes in the JET tokamak. *Physical Review Letters*, 134(9):095103, 2025.

[13] G. Brochard et al. Saturation of fishbone instability by self-generated zonal flows in tokamak plasmas. *Physical Review Letters*, 132(7):075101, 2024.

[14] S. Moradi et al. Core micro-instability analysis of JET hybrid and baseline discharges with carbon wall. *Nuclear Fusion*, 54(12):123016, 2014.

[15] N. Kumar et al. Turbulent transport driven by kinetic ballooning modes in the inner core of JET hybrid H-modes. *Nuclear Fusion*, 61(3):036005, 2021.

[16] S. Mazzi et al. Effects of kinetic ballooning modes on the electron distribution function in the core of high-performance tokamak plasmas. *Nuclear Fusion*, 65(1):016049, 2024.

[17] F. Jenko et al. Electron temperature gradient driven turbulence. *Physics of Plasmas*, 7(5):1904–1910, 2000.

[18] J. Citrin et al. Nonlinear stabilization of tokamak microturbulence by fast ions. *Physical Review Letters*, 111(15):155001, 2013.

[19] J. Garcia et al. Key impact of finite-beta and fast ions in core and edge tokamak regions for the transition to advanced scenarios. *Nuclear Fusion*, 55(5):053007, 2015.

[20] Ye. O. Kazakov et al. Physics and applications of three-ion ICRF scenarios for fusion research. *Physics of Plasmas*, 28(2):020501, 2021.

[21] M. Nocente et al. Generation and observation of fast deuterium ions and fusion-born alpha particles in JET D-^{3}He plasmas with the 3-ion radio-frequency heating scenario. *Nuclear Fusion*, 60(12):124006, 2020.

[22] H. Doerk et al. Gyrokinetic study of turbulence suppression in a jet-ilw power scan. *Plasma Physics and Controlled Fusion*, 58(11):115005, 2016.

[23] J. Varela et al. Stability optimization of energetic particle driven modes in nuclear fusion devices: the FAR3d gyro-fluid code. *Frontiers in Physics*, 12:1422411, 2024.

[24] J. Candy et al. A high-accuracy eulerian gyrokinetic solver for collisional plasmas. *Journal of Computational Physics*, 324:73–93, 2016.

[25] S. Mazzi et al. Study of fast-ion-driven toroidal alfvén eigenmodes impacting on the global confinement in TCV L-mode plasmas. *Frontiers in Physics*, 11:1225787, 2023.

[26] W. W. Heidbrink et al. Experimental studies of the interaction between fast ions, alfvén eigenmodes and fishbones, microturbulence, and zonal flows in the DIII-D tokamak. In *66th Annual Meeting of the APS Division of Plasma Physics, Atlanta, Georgia, USA, 7-11 October 2024*, 2024.

[27] J. Garcia et al. New H-mode regimes with small ELMs and high thermal confinement in the Joint European Torus. *Physics of Plasmas*, 29(3):032505, 2022.

[28] M. Fontana et al. High T_e discrepancies between ECE and thomson diagnostics in high-performance JET discharges. *Physics of Plasmas*, 30(12), 2023.

[29] V. Krivenski. Electron cyclotron emission by non-maxwellian bulk distribution functions. *Fusion Engineering and Design*, 53(1-4):23–33, 2001.

[30] L. Senni et al. Standardizing high electron temperature measurement comparisons: A method for cross-diagnostic and cross-machine analysis. *Journal of Instrumentation*, 20:C09009, 2025.